Measurement of the Higgs boson decay in $Z(ll)H, H \to WW$ at the FCC-ee at $\sqrt{s} = 240 GeV$

XXXIX Annual Meeting of the Division of Particles and Fields

J. Eysermans★, **Haydee Hernández-Arellano**†, F. Martínez†, I. Pedraza†

†Benemérita Universidad Autónoma de Puebla
Puebla, Puebla, México.
★Massachusetts Institute of Technology,
Cambridge, Massachusetts, USA.

May 22, 2025

Outline

1. FCC-ee: a Higgs factory
2. Relevance of $e^+e^- \to ZH$
3. Analysis of $e^+e^- \to Z(ll)H, H \to W(qq)W(qq)$
4. Results
5. Conclusions

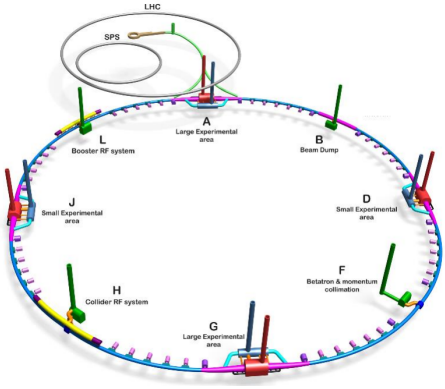

FCC opportunities*

- Map **Higgs and EW gauge boson properties** with unprecedented precision, probing interactions linked to the early universe ($10^{-12} - 10^{-10}$ s after the Big Bang).
- Improve knowledge of Standard Model phenomena (EW, QCD, flavour, Higgs, top) through **high-precision measurements**.
- Boost sensitivity to **rare low-energy processes**, including light, weakly coupled particles (e.g., neutrinos, axion-like particles), and decisively test dark matter candidates.
- Extend direct discovery reach for **new particles** by at least an order of magnitude at high energies.

*See more information at the **Future Circular Collider Feasibility Study Report**: Volume 1, Physics, Experiments, Detectors. DOI: 10.17181/CERN.9DKX.TDH9.

FCC-ee and FCC-hh

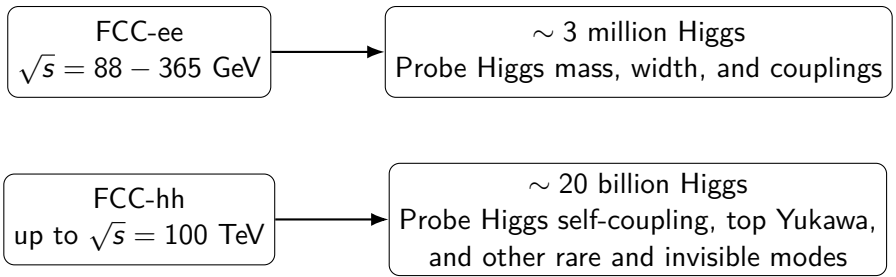

Higgs production from e^+e^- colliders at $\sqrt{s} = 240$ GeV

In e^+e^- collisions at $\sqrt{s} = 240$ GeV, Higgs are mainly produced through two modes: "Higgsstrahlung" and WW fusion process (VBF):

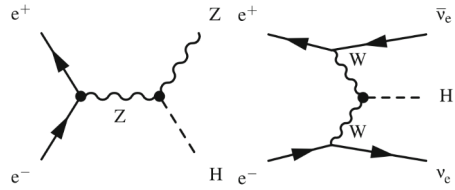

Higgs production modes for e^+e^- colliders at $\sqrt{s} = 240$ GeV *.

At the FCC-ee: significantly larger number of ZH events with a much smaller background will be observed compared with previous observations by ATLAS and CMS.

*Eysermans, J., & Selvaggi, M. (2025). DOI: 10.17181/9gzts-hsm97

Higgsstrahlung

Higgs model-independent studies can be carried out in Higgsstrahlung events: center-of-mass is known, information on the recoiling Higgs is accessible by the associated Z boson *.

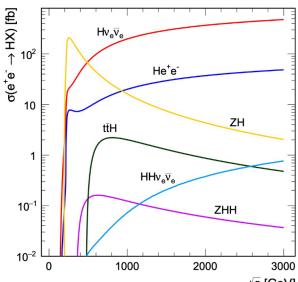

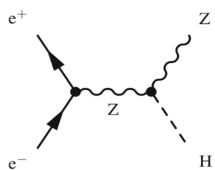

At $\sqrt{s} = 240$ GeV, the ZH rate is enhanced, sensitive to the *eeZ* and the *ZZH* vertices, along with the couplings to the Higgs. Images from: Sally Dawson, ZH at one loop in SMEFT

*Eysermans, J., Bernardi, G., Ang, L. (2025). DOI: 10.17181/jfb44-s0d81

Higgs couplings

From the Higgsstrahlung and WW fusion processses we can extract the different couplings of various Higgs decay modes ($H \to X\bar{X}$) using the following relations*:

$$\sigma_{ZH} \times Br(H \to X\bar{X}) \propto \frac{g^2_{HZZ} g^2_{HXX}}{\Gamma_H} \tag{1}$$

$$\sigma_{H\nu_e\nu_e} \times Br(H \to X\bar{X}) \propto \frac{g^2_{HWW} g^2_{HXX}}{\Gamma_H}$$

By analyzing the $H \to ZZ$ decay, we can extract the g_{HZZ} coupling from the first equation, which can then be used to obtain all other Higgs couplings for other decay channels.

*Eysermans, J., Bernardi, G., Ang, L. (2025). DOI: 10.17181/jfb44-s0d81

Other opportunities

Apart from determining the Higgs couplings with great precission, studying the ZH process will allow to

- Constraint the Higgs total width, by measuring the $H \to ZZ^*$ decay and the relation:

$$\Gamma_H \propto \frac{\sigma(e^+e^- \to ZH, H \to ZZ)^2}{\sigma(e^+e^- \to ZH}$$

- Probe the Higgs self-coupling through NLO deviations*:

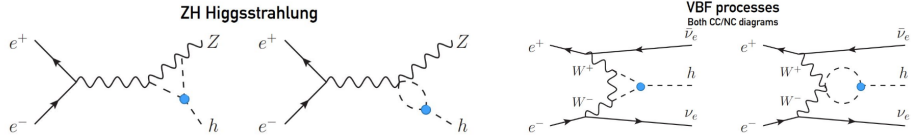

*Eysermans, J., Selvaggi, M. (2025) DOI:10.17181/9gzts-hsm97

$Z(\ell\ell)$ and $H \to WW$

- **Leptonic decays** of the Z boson $\to$ greater precision and efficient selection of the ZH events[a].
- **Mass recoil** against the lepton pair in the final state (m_{recoil}) $\to$ distinguish the ZH events from the main backgrounds ($WW, ZZ, Z\gamma$):

$$m^2_{recoil} = (\sqrt{s} - E_{\ell\ell})^2 - p^2_{\ell\ell} = s - 2E_{\ell\ell}\sqrt{s} + m^2_{\ell\ell} \quad (2)$$

- Our study will focus on the $H \to W^+W^-$ decay, particularly the **hadronic channel** ($\Gamma_{W,hadrons}/\Gamma_W \sim 67\%$).

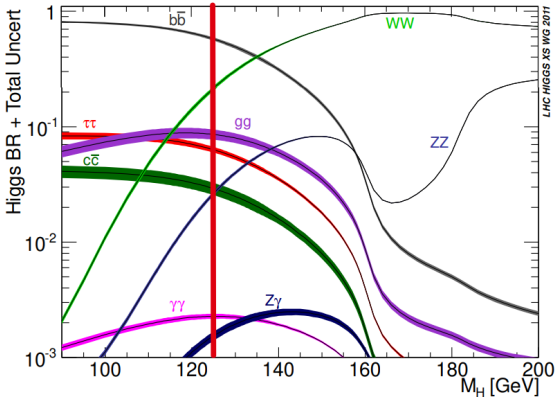

From: *Handbook of LHC Higgs Cross Sections*, DOI: 10.5170/CERN-2012-002

[a] Eysermans, J., Bernardi, G., Ang, L. (2025). DOI: 10.17181/jfb44-s0d81

Final State of the Studied Process

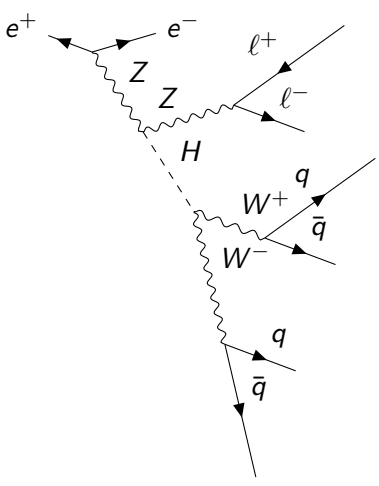

We study the process
$e^+e^- \to ZH \to Z(\ell^+\ell^-)H(W^+W^-) \to Z(\ell^+\ell^-)W(qq)W(qq)$.
For the final state we look for events with:

1. Two opposite-charged electrons/muons.
2. At least one isolated, with p>20 GeV.
3. Four jets.

Signal and Background Samples

Monte Carlo event samples generated with WHIZARD and PYTHIA8, passed through a parametric simulation of the IDEA detector using DELPHES (winter2023 campaign).

Process	Simulation Label	$\sigma[fb]$	Events Generated
Signal:			
$e^+e^- \to Z(\mu\mu)H,\ H \to WW$	wzp6_ee_mumuH_HWW_ecm240	1.456	400,000
$e^+e^- \to Z(ee)H,\ H \to WW$	wzp6_ee_eeH_HWW_ecm240	1.541	400,000
Background:			
$e^+e^- \to ZZ$	p8_ee_ZZ_ecm240	1358.99	11,300,000
$e^+e^- \to WW$	p8_ee_WW_ecm240	16438.5	74,728,800
$e^+e^- \to Z(\mu\mu)\gamma$	wzp6_ee_mumu_ecm240	5288	10,700,000
$e^+e^- \to ee$	wzp6_ee_ee_Mee_30_150_ecm240	8305	85,400,000
$e^+e^- \to Z(\mu\mu)H,\ H \to ZZ$	wzp6_ee_mumuH_HZZ_ecm240	0.1786	400,000
$e^+e^- \to Z(ee)H,\ H \to ZZ$	wzp6_ee_eeH_HZZ_ecm240	0.1891	400,000
$e^+e^- \to Z(qq)H,\ H \to ZZ$	wzp6_ee_qqH_HZZ_ecm240	1.409	1,200,000
$e^+e^- \to Z(bb)H,\ H \to ZZ$	wzp6_ee_bbH_HZZ_ecm240	0.7915	1,000,000
$e^+e^- \to Z(cc)H,\ H \to ZZ$	wzp6_ee_ccH_HZZ_ecm240	0.6164	1,200,000
$e^+e^- \to Z(ss)H,\ H \to ZZ$	wzp6_ee_ssH_HZZ_ecm240	0.7912	600,000

$Z(l^+l^-)H$ event selection: kinematic cuts

1. 2 op. ch. muons, $p > 20$ GeV, at least one isolated
2. Veto on ℓ's with $5 < p < 20$ GeV
3. $m_{\ell\ell} \in [86, 96]$ GeV, $p_{\ell\ell} \in [30, 57]$ GeV
4. $|\cos\theta_{miss}| < 0.98$

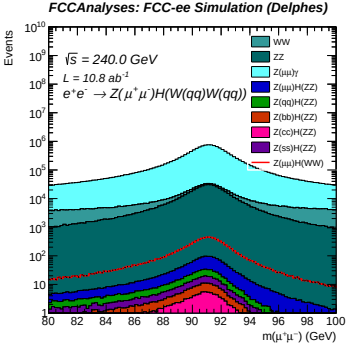

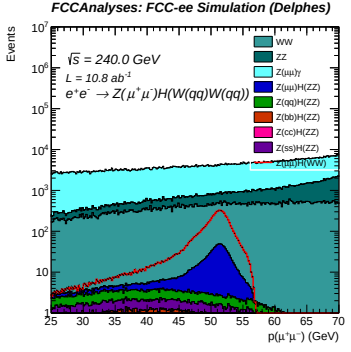

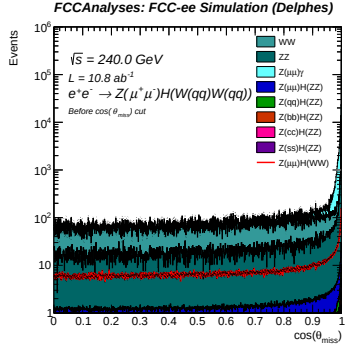

Jet Clustering and Di-Jet Pair Selection

- Restrict the $W \to \ell\nu$ decays by cuting events with missing energy $E_{miss} > 10$ GeV.
- Create a collection of particles removing both muons and electrons with $p > 20$ GeV.
- Exclusive $N = 4$ "Durham" algorithm is used for jet clustering, which is a sequential spherical k_t clustering method[a].

[a] S. Catani et al Physics Letters B, 269(3):432–438, 1991

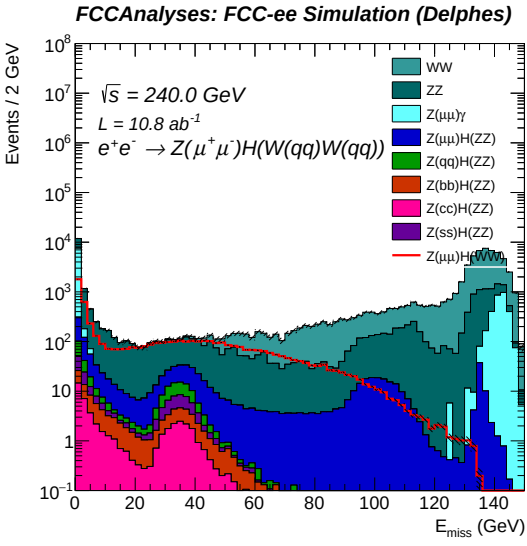

Jet Clustering and Di-Jet Pair Selection

We choose the best dijet pair to reconstruct the two W bosons by maximizing[a] :

$$P_W^{jj} = \frac{M_W^2 \Gamma_W^2}{\left(m_{jj}^2 - M_W^2\right)^2 + M_W^2 \Gamma_W^2}. \qquad (3)$$

- $jj[0]$: Maximizing pair (*"on-shell"*).
- $jj[1]$: The remaining pair (*"off-shell"*).

Same procedure but with M_Z and Γ_Z instead: use the resulting dijet-pair invariant mass ($m_{jj[0]}^Z$) to further reduce the ZZ background.

[a] Piotr Niezurawski et al JHEP11(2002)034

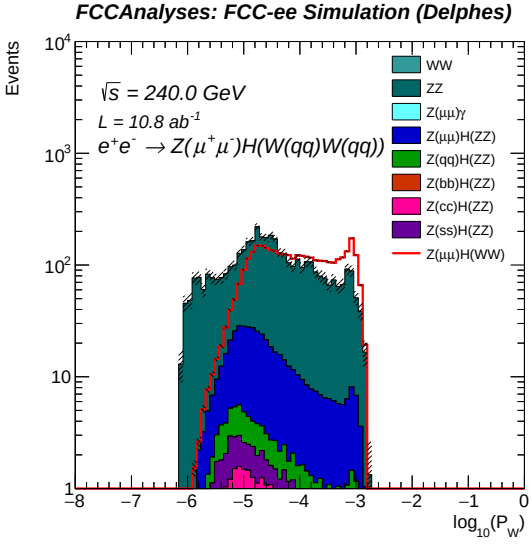

Final Selection Cuts

- Cut 1: Events with only two opposite charge $\mu's$.
- Cut 2: Veto on $\mu's$ and $e's$ with momentum within $[5, 20]$ GeV.
- Cut 3: $86 < m_{\mu\mu} < 89$ GeV.
- Cut 4: $30 < p_{\mu\mu} < 57$ GeV.
- Cut 5: $|\cos\theta_{miss}| < 0.98$.
- Cut 6: Missing energy $E_{miss} < 10$ GeV.
- Cut 7: $n_{jet} = 4$.
- Cut 8: $125 < E_{visible}^{\text{no Z}} < 145$ GeV, where $E_{visible}^{\text{no Z}}$ is the visible energy of the particles excluding the two Z muons.
- Cut 9: $120 < m_{4j} < 130$ GeV, where m_{4j} is the four-jet invariant mass.
- Cut 10: $m_{jj[1]} > 15$ GeV and $\Delta R_{jj[1]} > 0.4$, where $m_{jj[1]}$ is the invariant mass of the off-shell-W jet pair, and $\Delta R_{jj[1]}$ is the corresponding ΔR.
- Cut 11: $log_{10} P_W > -5.2$, where P_W is the quantity described previously.
- Cut 12: $m_{jj[0]}^{Z} < 89$ GeV, where $m_{jj[0]}^{Z}$ is the invariant mass of the on-shell dijet pair selected to align to the mass of the Z boson.

$Z(l^+l^-)H, H \to W(qq)W(qq)$ Cut Flow

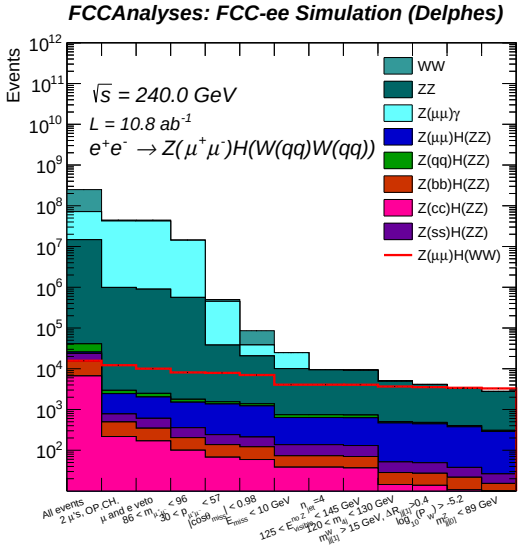

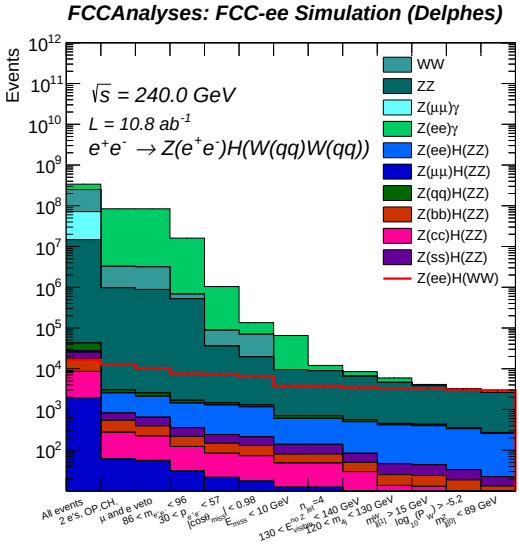

Final Results: Fit to recoil mass after selections

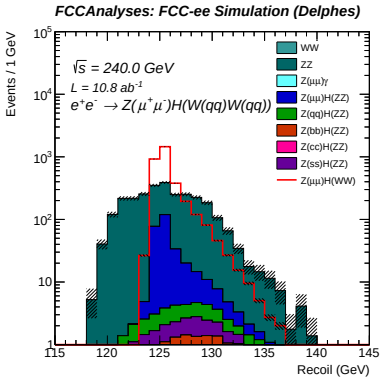

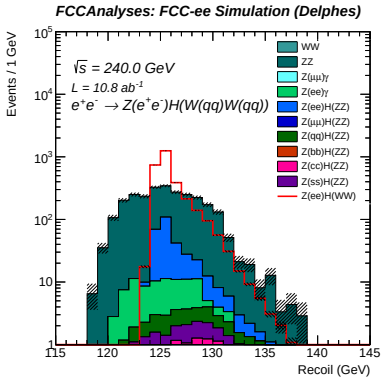

Uncertainty after best-fit (with log-normal uncertainty of 3% for $H \to ZZ$ background and 1% for the rest):

- $\mu^+\mu^-$ channel: 2.15.
- e^+e^- channel: 2.30.

The uncertainty for the combined contributions is 1.60**.**

Results in Technical Note (DOI:10.17181/x48j4-3kg84) part of the Future Circular Collider Feasibility Study Report, to be presented to the European Strategy for Particle Physics (ESPP).

Conclusions

- We have evaluated the **sensitivity of the measurement** of the Higgs boson branching ratio to the hadronic decay mode of the W^+W^- final state at the Future Circular Collider.
- The signal was extracted via a **binned likelihood fit** to the recoil mass distribution, utilizing the Combine tool. The fit was applied across the full range of the recoil mass, with a bin width of 1 GeV.
- The uncertainties in the measured branching ratio for the $H \to W^+W^-$ hadronic decay mode were found to be 2.15 and 2.30 for the $Z(\mu\mu)$ and $Z(ee)$ channels, respectively, with a **combined uncertainty of** 1.60.
- These results highlight the potential of the Future Circular Collider to provide a **precise determination of the Higgs branching ratio** to a pair of W bosons, with minimal uncertainty.

References I

[1] M. Benedikt et al. Future Circular Collider Feasibility Study Report: Volume 1, Physics, Experiments, Detectors. 4 2025. doi: 10.17181/CERN.9DKX.TDH9.

[2] Jan Eysermans and Michele Selvaggi. Total zh hadronic cross-section at fcc-ee and combination with leptonic final states, March 2025. URL https://doi.org/10.17181/e9wsh-tb178.

[3] Jan Eysermans, Gregorio Bernardi, and Li Ang. Higgs boson mass and model-independent zh cross-section at fcc-ee in the di-electron and di-muon final states, March 2025. URL https://doi.org/10.17181/c5dn3-c0s73.

[4] S. Catani, Yu.L. Dokshitzer, M. Olsson, G. Turnock, and B.R. Webber. New clustering algorithm for multijet cross sections in e+e− annihilation. *Physics Letters B*, 269(3):432–438, 1991. ISSN 0370-2693. doi: https://doi.org/10.1016/0370-2693(91)90196-W. URL https://www.sciencedirect.com/science/article/pii/037026939190196W.

[5] Piotr Niezurawski, Aleksander Filip Zarnecki, and Maria Krawczyk. Study of the higgs-boson decays into w +w − and zz at the photon collider. *Journal of High Energy Physics*, 2002(11):034, dec 2002. doi: 10.1088/1126-6708/2002/11/034. URL https://dx.doi.org/10.1088/1126-6708/2002/11/034.

THANK YOU!

Back-up Slides

Multivariate Analysis and BDT training

The classification of signal events in the $Z(\ell\ell)H, H \to WW$ process at FCC-ee is performed using a Multivariable Analysis (MVA) approach based on Boosted Decision Trees (BDT), implemented via the XGBoost library.

Features:

- **Four-jet invariant mass:** *jj_m_4jet*,
- **On-shell-W dijet invariant mass:** *jj_m_ww_1*,
- **Off-shell-W dijet invariant mass:** *jj_m_ww_2*,
- **Probability of dijet pairings to correspond to the W boson:** *PW* ,
- **On-shell-Z dijet invariant mass:** *jj_m_zz_1*,
- **Off-shell-Z dijet invariant mass:***jj_m_zz_2*
- $Z_{\mu\mu}$ **kinematics:** momentum (*zmumu_p*) and $\Delta\phi$ (*zmumu_deltaphi*).
- **Visible energy (excluding Z muons):** *visible_energy*.
- **On-shell-W and Off-shell-W dijet pairs separation:** ΔR_1 (*DeltaR_1*), ΔR_2 (*DeltaR_2*), respectively.

Hyperparameters:

- `objective`: `binary:logistic`
- `eval_metric`: `auc`
- `eta`: 0.1
- `max_depth`: 5
- `subsample`: 0.5
- `colsample_bytree`: 0.5
- `n_estimators`: 350
- `learning_rate`: 0.20
- `gamma`: 3
- `min_child_weight`: 10
- `early_stopping_rounds`: 25

BDT variable scores

Scores for each of the features chosen for the clasifier in the BDT training. A higher score suggests that the variable is more valuable for classification purposes.

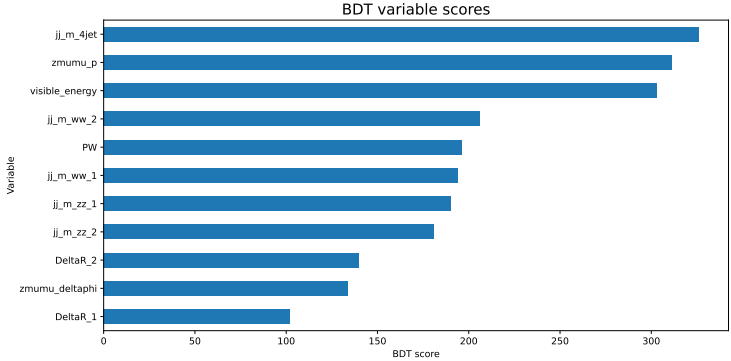

ROC Curve

Receiver Operating Characteristic (ROC) curve. In our case, the value of the Area Under the Curve (AUC) indicates that the ability of the model to distinguish between signal and background is acceptable (above 0.9).

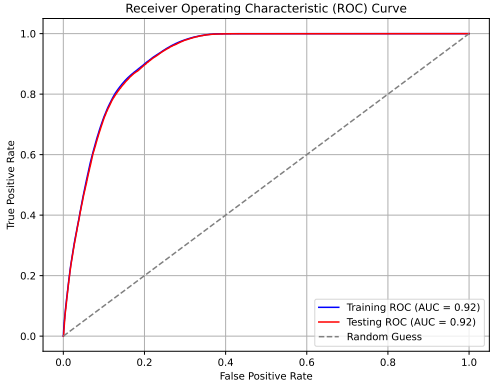

BDT Score Distribution

Distribution of the scores produced by the BDT classifier for the signal (blue) and background (red).